Cost-Aware Renewable Energy Management: Centralized vs. Distributed Generation

Johann Leithon*

Department of Signal Processing and Acoustics, Aalto University, e-mail: johann.leithon@aalto.fi

Stefan Werner

Department of Electronic Systems, Norwegian University of Science and Technology, e-mail: stefan.werner@ntnu.no.

Visa Koivunen

Department of Signal Processing and Acoustics, Aalto University, e-mail: visa.koivunen@aalto.fi

Abstract

We propose optimization strategies for cooperating households equipped with renewable energy assets and storage devices. We consider two system configurations: In the first configuration, households share access to an energy farm, where electricity is generated from renewable sources and stored in battery banks. In the second configuration, households are equipped with their own renewable energy sources and storage devices, and are allowed to share energy through the grid. The developed optimization model takes into account location and time-varying energy prices as well as energy transfer fees. To design our strategies, we first establish performance bounds, and compare the two configurations in terms of achievable savings and usability of renewable energy. Then, we devise real-time energy management algorithms by incorporating forecasting techniques in the proposed framework. Simulation results show that the proposed strategies outperform existing solutions by up to 10%. It is also shown that cooperative strategies outperform greedy approaches by up to 6.8%.

☆This work was supported in part by the Academy of Finland under Grant 296849.

*Corresponding author

Keywords: Energy storage, energy allocation, cooperative strategies, non-convex optimization.

1. Introduction

Renewable energy generators can be deployed by end users to lower their electricity bills [1–3], support load balancing applications [4], and reduce their carbon footprint. To handle the intermittency of the renewable energy source, energy storage devices can be used to enhance the utility of the renewable energy over specific planning periods [5–7]. Storage devices can also be used to solve over-voltage issues caused by a high renewable energy penetration [8].

To further enhance the utility of local renewable energy, cooperative schemes, such as Shared Solar[1] can be used to leverage geographic diversity and minimize the upfront investment. In a cooperative environment, where participants share energy to minimize their collective expenditure and/or carbon emissions, renewable energy generators and storage devices can be deployed in different configurations [10].

In this paper, we propose cooperative strategies that minimize the energy expenditure incurred by the participating households over a finite planning horizon. The novelty of the approach proposed in this paper in comparison to existing methods is as follows: First, we develop and compare two approaches to cooperative energy management, namely centralized and distributed renewable energy generation. We approach the problem from the perspective of the consumers, not the utility company. Second, our modelling framework focuses on optimizing renewable energy allocation across cooperating households and energy consumption over time. Moreover, the households' loads are assumed non-deferrable (inflexible), thus ensuring full user satisfaction over the entire planning period. Third, our proposed real-time algorithms have the following advantages over existing strategies:

[1] Community Shared Solar is a "solar-electric system that provides power and/or financial benefit to multiple community members" [9].

- The computational complexity of the proposed forecasting-based real-time algorithms can be controlled by varying the rate at which the forecasts and decision variables are updated.

- The proposed forecasting-based real-time algorithms are not restricted to a particular renewable energy generation model, or a particular energy consumption model. Contrarily, different statistical models can be considered and hence, the algorithm can be applied in different scenarios.

- By using the proposed forecasting-based real-time algorithms, we can improve the prediction accuracy on a continuous basis. Measurements are acquired in each time slot and they can be used for model identification, which in turn can enhance the statistical understanding of the stochastic processes that model renewable energy generation and household power consumption.

- The proposed algorithms allow us to exploit seasonality effects, trends, and other characteristics of non-stationary stochastic processes that model renewable energy generation and power consumption. For example, historical records can be used to build time series models which can capture characteristics such as seasonality in renewable energy generation data.

This paper is organized as follows. The literature review is presented in Sec. 2. The system model is explained in Sec. 3. We derive the optimal energy management strategy for the configuration with centralized renewable energy generation (CREG) in Sec. 4. The proposed strategy for the configuration with distributed renewable energy generation (DREG) is presented in Sec. 5. A comparison between the two renewable energy production configurations is presented in Sec. 6. The proposed real-time algorithms are presented in Sec. 7. Numerical results are discussed in Sec. 8, and conclusions are presented in Sec. 9.

Nomenclature

Table 1: Main variables and their notation

$\boldsymbol{\ell}_m$	Power consumed by the mth household
$\boldsymbol{p}_m$	Energy prices offered to the mth household
$\boldsymbol{d}_m$	Renewable power drawn by the mth household
$\boldsymbol{j}$	Renewable energy available at the energy farm
$\boldsymbol{j}_m$	Renewable energy available at the mth household
$\boldsymbol{r}_m$	Renewable power generated at the mth household
$\pi_{\mathsf{orig},\mathsf{des}}(n)$	Renewable power transferred from household orig to household des, nth time slot
$\boldsymbol{\gamma_m}$	Total renewable power received by household m from others
$\boldsymbol{\theta}_m$	Total renewable power transferred from household m to others
α	Charging efficiency rate, battery bank at energy farm
β	Discharging efficiency rate, battery bank at energy farm
α_m	Charging efficiency rate, battery at household m
β_m	Discharging efficiency rate, battery at household m
Δt	Time step, time difference between consecutive samples
Ψ	Storage capacity, battery bank at energy farm
Ψ_m	Storage capacity, battery at household m
q_C	Maximum charging rate, battery bank at energy farm
q_D	Maximum discharging rate, battery bank at energy farm
$q_{C,m}$	Maximum charging rate, battery at household m
$q_{D,m}$	Maximum discharging rate, battery at household m
$\boldsymbol{r}$	Renewable power generated at the energy farm over time
$\boldsymbol{r}_m$	Renewable power generated at household m over time
χ	Total energy cost incurred by participating households
$\otimes$	Kronecker product
$\mathbf{A}_N$	$N \times N$ lower triangular matrix of ones
$\mathbf{1}_{N,M}$	$N \times M$ matrix of ones
$\mathbf{0}_{N,M}$	$N \times M$ matrix of zeros
$\preceq$	Element-wise less than or equal to
$\Pi(:,:,:)$	Power transfer tensor, with $\Pi(n, \mathsf{orig}, \mathsf{des}) = \pi_{\mathsf{orig},\mathsf{des}}(n)$
ϵ	Cost of transferring energy within planning horizon
ϕ	Parameter used to represent different transfer fees
REU_C	Renewable energy left unused, centralized configuration
REU_D	Renewable energy left unused, distributed configuration

In this paper column vectors are presented with lower case bold letters. Matrices are represented with upper case bold letters. Scalars are represented by regular fonts. The nth element of vector $\mathbf{j}$ is denoted by $j(n)$. The $N \times M$ matrices of zeros and ones are respectively denoted by $\mathbf{0}_{N,M}$ and $\mathbf{1}_{N,M}$. The $N \times N$ identity matrix is denoted by $\mathbf{I}_N$. Also, $\otimes$ denotes the Kronecker product, $\preceq$ denotes element-wise $\leq$, and $a(n)$ is the nth element of vector $\boldsymbol{a}$. The notation of the most important variables in the system model is presented in Table 1.

2. Related Works

Energy management in buildings and households has been studied extensively. Most of the recent works in this area focus on scheduling deferrable appliances to minimize the household's energy cost incurred over specific planning periods, see, e.g., [11–15]. In [11] and [13] comfort constraints are imposed to ensure a satisfactory user experience. Some works consider loads that are not always present in the building/house such as electrical vehicles [12]. Works such as [14] and [15] account for storage devices as well.

Strategies that enable integration of renewable energy into the grid through storage management, demand response,[2] or power balancing can be found in [17, 18] and [19]. Papers [3] and [20] propose suboptimal energy management strategies based on evolutionary algorithms. Similarly, a battery management strategy based on neural[3] networks and dynamic programming[4] is presented in [21]. The proposed strategy aims at minimizing the energy cost through renewable energy and storage management. However, the solution presented in [21] is approximate and only converges in a few scenarios.

Solutions based on game theory are proposed in several works, e.g., see [22]

[2] Demand response programs seek to modify energy consumption patterns through economic incentives [16].

[3] A neural network is a parametrized model, which is used to make predictions. Its parameters are optimized to maximize its accuracy on a training set.

[4] Dynamic programming is an optimization framework, which breaks problems into simpler subproblems and uses recurrence to find a solution.

and [23]. These solutions are meant to balance the priorities of game participants such as utility companies and consumers. A renewable energy trading system is studied in [24], where strategies are proposed to maximize the profit of an *energy harvesting company* through renewable energy management.

Energy management solutions for microgrids[5] are proposed in [25–28] and [29]. Most of these strategies are designed to minimize the operational cost of microgrids over finite planning horizons. Some works, e.g. [25], develop strategies to maximize the utility of the energy consumed over the specified optimization period. Works such as [26] take into consideration the maintenance cost of the storage device. The physical aspects of the energy management problem are investigated in [30] and [31], where the authors propose schemes to enhance the deployment of energy management strategies in practical scenarios.

Related works on cooperative energy management include [10, 32–40]. In [32], a technique is proposed to solve the economic dispatch problem in a decentralized manner assuming information cooperation across distributed power systems. Works such as [33] and [35] present strategies to reduce grid losses by scheduling loads (among participating households) or power flows (among microgrids). In [34], a strategy is proposed to reduce load disconnection. The cooperative strategies proposed for microgrids in [10, 36, 37, 40] only consider a configuration with distributed renewable energy generation. In general, these strategies are designed to optimize the operation of the grid/distribution system, or reduce the generation cost incurred by the utility.

Real-time energy management strategies have been proposed in works such as [41–52], and [53], where the authors develop frameworks to optimize energy assets in real time. In [42], the proposed strategies aim at minimizing both the energy costs and the thermal discomfort. In [41, 42, 47] and [48] the proposed strategies are meant to optimize the average performance of the system. The algorithms proposed in [46] and [53] are meant for use in data centers, while

[5] A microgrid is an energy ecosystem composed of energy sources and loads, and confined to a defined geographical area.

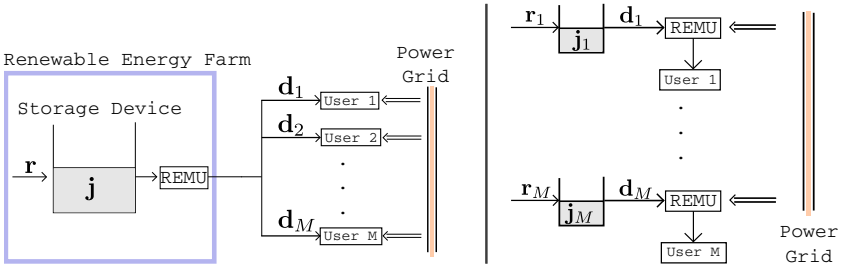

Figure 1: Left: CREG. Right: DREG. REMU stands for renewable energy management unit.

the framework in [52] is meant to optimize the charging operations in electrical vehicles.

The strategy proposed in [49] is based on game theory and does not account for time-varying electricity prices. In [50], the strategy proposed aims at minimizing both energy costs and polluting gas emissions. However, the strategy developed in [50] is not cooperative in nature, as it only assumes a single energy source. In [54] the authors propose an architecture for real-time management that accounts for renewable energy assets. However, the proposal developed in [54] only concerns economic optimization for generation-side management, and as such, it targets utility companies and grid operators.

Unlike existing solutions, in this paper we consider location- and time-varying electricity prices, loads, and renewable energy generation profiles. The energy prices are dynamic and made known in advance to the users, as part of a demand response program [55]. The developed optimization framework also accounts for parameterized energy transfer fees, thus allowing utilities and grid operators charge for power transferring operations across households. Finally, our framework accounts for non-deferrable (inflexible) loads, thus ensuring full user satisfaction over the entire planning period.

3. System Model

3.1. Loads, Planning Horizon, Objective, and Design Variables

We consider a set of M grid-tied households, and seek to minimize their collective energy expenditure over a finite planning horizon of N time slots, each one of duration Δt. Each household is permanently connected to the grid, and is subject to different energy consumption patterns. The power consumed by the mth household in the nth time slot is denoted by $\ell_m(n),\ n \in \{1, \ldots, N\}$, and is non-deferrable in order to ensure total user satisfaction over the planning period. The decision variables are the charging/discharging schedules of the storage devices. They thus determine the optimal power that should be drawn from the grid in order to minimize the total cost incurred by the participating households.

3.2. Renewable Energy Production and Storage Configurations

We consider two system configurations, namely a system with centralized renewable energy generation (CREG), and a system with distributed renewable energy generation (DREG). These two configurations are illustrated in Fig. 1. As seen in Fig. 1, each configuration requires a different storage arrangement. That is, in CREG the storage devices are all placed in a single location (the generation site), whereas, in DREG, the storage devices are placed across different households. The configuration with distributed renewable energy generation can be found in most countries around the world, whereas the configuration with centralized renewable energy generation is becoming popular among households with insufficient space to deploy renewable energy generators and in communities where consumers want to reduce capital investment.

3.2.1. CREG

In this configuration, the households share access to an energy farm, where renewable energy is generated and stored. The energy farm is composed of energy harvesting devices such as solar panels or windmills, and energy storage devices such as battery banks. The renewable power drawn from the energy

farm by the mth household is denoted by $\boldsymbol{d}_m \in \mathbb{R}_+^N$. Hence, the power drawn from the grid by the mth household is $\boldsymbol{\ell}_m - \boldsymbol{d}_m$, where $\boldsymbol{d}_m$ must satisfy:

$$d_m(n) \leq \ell_m(n), \ \forall \ n. \tag{1}$$

3.2.2. DREG

In this configuration, each household is equipped with its own renewable energy generator and storage device. To minimize their collective energy expenditure, households share renewable energy through the grid thus incurring transfer fees. The renewable power transferred from the storage device at household $\mathsf{orig} \in \{1, \ldots, M\}$ to the storage device at household $\mathsf{des} \in \{1, \ldots, M\}$ is denoted by $\pi_{\mathsf{orig},\mathsf{des}}(n)$, the total renewable power received by household des from others is denoted by $\boldsymbol{\gamma}_{\mathsf{des}} \in \mathbb{R}_+^N$. Similarly, the total renewable power transferred from household orig to other households is denoted by $\boldsymbol{\theta}_{\mathsf{orig}} \in \mathbb{R}_+^N$. The vectors $\boldsymbol{\gamma}_{\mathsf{des}}$ and $\boldsymbol{\theta}_{\mathsf{orig}}$ can be written in terms of $\pi_{\mathsf{orig},\mathsf{des}}(n)$ as follows:

$$\gamma_{\mathsf{des}}(n) = \sum_{\mathsf{orig} \neq \mathsf{des}}^{M} \pi_{\mathsf{orig},\mathsf{des}}(n), \ \theta_{\mathsf{orig}}(n) = \sum_{\mathsf{des} \neq \mathsf{orig}}^{M} \pi_{\mathsf{orig},\mathsf{des}}(n), \ \forall \ n. \tag{2}$$

By the energy conservation principle, we have the following balancing requirement for $\boldsymbol{\gamma}_m$ and $\boldsymbol{\theta}_m$:

$$\sum_{m=1}^{M} \gamma_m(n) = \sum_{m=1}^{M} \theta_m(n), \ \forall \ n, \tag{3}$$

which states that the energy delivered is equal[6] to the energy received by the households in each time slot.

3.3. Energy Storage Devices

The storage devices[7] in both configurations are characterized by the following properties:

[6] The transfer losses are absorbed by the grid operator or utility, and are accounted for in the transfer fee.

[7] In this paper we use the term storage device to refer to a system composed of potentially multiple energy storage devices, such as a battery bank.

3.3.1. Charging/discharging losses

Each storage device in the system is subject to charging/discharging losses, which are proportional to the power charged to or discharged from the storage device. The storage device charging/discharging efficiency rates at the energy farm are respectively denoted by α and β, and satisfy $0 < \alpha \leq 1$ and $0 < \beta \leq 1$. A lossless charging (discharging) operation takes place when $\alpha = 1$ ($\beta = 1$). The storage device charging/discharging efficiency rates at the mth household are respectively α_m and β_m, which also satisfy $0 < \alpha_m \leq 1$ and $0 < \beta_m \leq 1$. Again, a lossless charging (discharging) operation happens when $\alpha_m = 1$ ($\beta_m = 1$).

3.3.2. Storage device dynamics

The energy available in the storage device at the energy farm is denoted by $\boldsymbol{j} \in \mathbb{R}_+^N$, and satisfies:

$$j(\eta) = j(0) + \Delta t \sum_{n=1}^{\eta} \left[\alpha c(n) - \frac{1}{\beta} \sum_{m=1}^{M} d_m(n) \right], \tag{4}$$

where $j(0) \geq 0$ is the energy initially available in the storage device, $\eta \in \{1, \ldots, N\}$, and $c(n)$ is the total renewable power charged into the storage device during the nth time slot. Similarly, the energy available in the storage device at the mth household is denoted by $\boldsymbol{j}_m \in \mathbb{R}_+^N$, and evolves according to:

$$j_m(\eta) = j_m(0) + \Delta t \sum_{n=1}^{\eta} \left[\alpha_m c_m(n) - \frac{1}{\beta_m} \left[d_m(n) + \theta_m(n) \right] \right], \tag{5}$$

where $j_m(0) \geq 0$ is the energy initially available in the mth storage device, and $\boldsymbol{c}_m \in \mathbb{R}_+^N$ and $\boldsymbol{d}_m \in \mathbb{R}_+^N$ are, respectively, the renewable power charged to, and discharged from the mth storage device.

3.3.3. Limited storage capacity

The capacity of the storage device at the energy farm is denoted by $\Psi \in \mathbb{R}_+$, and the capacity of the storage device at the mth household is denoted by $\Psi_m \in \mathbb{R}_+$. Therefore, $c(n)$, $c_m(n)$, and $d_m(n)$, $m \in \{1, \ldots, M\}$ must be such that:

$$0 \leq j(n) \leq \Psi, \forall\, n \in \{1, \ldots, N\}, \tag{6}$$

and

$$0 \leq j_m(n) \leq \Psi_m, \forall\ n\ \in\ \{1, \ldots, N\}. \tag{7}$$

3.3.4. Limited charging/discharging rate

Each storage device has a limited charging/discharging rate, expressed as the maximum amount of energy that can be injected to, or drawn from the storage device in each time slot. The maximum charging (discharging) rate that the storage device at the energy farm can handle is q_C (q_D) power units. These limitations impose the following constraints on $c(n)$ and $d(n) \triangleq \sum_{m=1}^{M} d_m(n), \forall\ n$:

$$c(n) \leq q_C,\ d(n) \leq q_D,\ \forall\ n\ \in\ \{1, \ldots, N\}. \tag{8}$$

Similarly, the maximum charging (discharging) rate that the storage device at the mth household can handle is $q_{C,m}$ ($q_{D,m}$) power units. Therefore,

$$c_m(n) \leq q_{C,m},\ d_m(n) + \theta_m(n) \leq q_{D,m},\ \forall\ m,\ \forall\ n. \tag{9}$$

3.4. Renewable Energy Generation

The total renewable energy generated at the energy farm is denoted by $\boldsymbol{r}\ \in\ \mathbb{R}_+^N$, whereas the renewable energy generated at the mth household is $\boldsymbol{r}_m\ \in\ \mathbb{R}_+^N$. Therefore, the power charged into the storage device at the energy farm satisfies:

$$c(n) \leq \min\{q_C, r(n)\},\ \forall\ n. \tag{10}$$

Similarly, the power charged into the storage device at the mth household satisfies:

$$c_m(n) \leq \min\{q_{C,m}, r_m(n) + \gamma_m(n)\},\ \forall\ n, \forall\ m, \tag{11}$$

where $\gamma_m(n)$, defined in (2), is the total renewable power received by the mth household from other cooperating households.

3.5. Pricing Scheme

To ensure generality, we consider location- and time-varying electricity prices. That is, each household is subject to potentially different pricing signals. The cost of the energy consumed by the mth household over the N-slot planning period is

$$\xi_m = \sum_{n=1}^{N} p_m(n) \left[\ell_m(n) - d_m(n)\right] \Delta t, \tag{12}$$

where $\boldsymbol{p}_m \in \mathbb{R}_+^N$ denotes the energy prices, and $\boldsymbol{d}_m$ satisfies (1). The cost of the energy consumed by the entire group of households is thus

$$\chi = \sum_{m=1}^{M} \xi_m. \tag{13}$$

In the following sections we formulate two optimization problems, which we solve to determine the energy management strategy that minimizes χ in the configurations described in Sec. 3.2. The savings obtained can be allocated to participants following different policies, e.g., in proportion to their initial investment or their renewable energy generation capacity.

4. Centralized renewable energy Generation (CREG)

In this section we analyse the configuration with CREG. We start by formulating an optimization problem to minimize the energy cost incurred by all the participating households. Then we solve the optimization problem by assuming full knowledge of the renewable energy generation and the energy consumption profiles over the entire planning horizon. The obtained energy management strategy is thus genie-aided and serves as a performance benchmark for any real-time algorithm. In Sec. 7 we will explain how forecasting techniques can be incorporated in the proposed strategy for its implementation in real time.

4.1. Problem Formulation

With CREG, the decision variables are the power discharged from the energy farm by each household, and denoted by $\boldsymbol{d}_m$'s, and the power charged into

the centralized storage device, and denoted by $\boldsymbol{c}$. Therefore, the optimization problem can be formulated as follows:

$$\begin{aligned} \text{P0:} \quad & \min_{\boldsymbol{c},\, \boldsymbol{d_1}, \ldots, \boldsymbol{d_M}} \ \chi \\ \text{s.t.} \quad & (1),\ (6),\ (8),\ \text{and}\ (10). \end{aligned} \tag{14}$$

In P0, $\boldsymbol{j}$ and the $\boldsymbol{d}_m$'s are connected through (4). P0 is a convex optimization problem because the objective is linear and the design space is convex. Moreover, P0 can be cast as a standard linear programming problem by using appropriate substitutions as shown in Sec. 4.2.

4.2. Solution Strategy

In this section we show how P0 can be formulated as a standard linear program. We first introduce some definitions to simplify notation. Let

$$\mathbf{G} = [\alpha \Delta t \mathbf{A}_N \qquad -\frac{1}{\beta}\Delta t \mathbf{1}_{1,M} \otimes \mathbf{A}_N], \tag{15}$$

where $\mathbf{A}_N$ is the $N \times N$ lower triangular matrix of ones. Clearly, $\mathbf{G}$ is an $N \times (N + NM)$ matrix. By using $\mathbf{G}$, constraint (6) can be written compactly as follows:

$$\mathbf{0}_{N,1} \preceq \mathbf{G} \begin{pmatrix} \mathbf{c} \\ \mathbf{d}_1 \\ \mathbf{d}_2 \\ \vdots \\ \mathbf{d}_M \end{pmatrix} \preceq [\Psi - j(0)]\, \mathbf{1}_{N,1}. \tag{16}$$

After introducing the definitions described above, P0 can be cast as a linear programming problem and solved by using standard techniques such as the Karmarkar's algorithm. P0 can be cast as a linear programming problem because its feasibility space is determined by linear inequalities, and its objective is an affine function of the decision variables. Karmarkar's algorithm can solve linear programming problems in polynomial time [56], and is implemented in programming packages for numerical computation such as Scilab [57].

5. Distributed renewable energy Generation (DREG)

In this section we analyse the configuration with DREG. We first formulate an optimization problem to minimize the energy cost incurred by all the participating households over the specified planning horizon. Given the complexity of the problem, we derive alternative formulations and use a combination of techniques to solve the original optimization problem. The obtained energy management strategy is genie-aided, as it requires full knowledge of the variables involved in the problem. The strategy proposed can then be used to benchmark real-time algorithms. In Sec. 7 we will incorporate forecasting techniques to enable the practical implementation of the proposed strategy.

5.1. Power Transfer Tensor

With DREG, the decision variables are the $\boldsymbol{c}_m$'s, the $\boldsymbol{d}_m$'s, and the power transfer tensor $\mathbf{\Pi} \in \mathbb{R}_{+}^{N \times M \times M}$, which is defined as follows:

$$\Pi(n,:,:) = \begin{pmatrix} \pi_{1,1}(n) & \pi_{1,2}(n) & \dots & \pi_{1,M}(n) \\ \pi_{2,1}(n) & \pi_{2,2}(n) & \dots & \pi_{2,M}(n) \\ \vdots & \vdots & \ddots & \vdots \\ \pi_{M,1}(n) & \pi_{M,2}(n) & \dots & \pi_{M,M}(n) \end{pmatrix}, \tag{17}$$

where $n \in \{1,\dots,N\}$. Recall that $\pi_{\mathsf{orig},\mathsf{des}}(n)$ is the renewable power transferred in the nth time slot from the storage device at household orig to the storage device at household des. Since the power exchange cannot happen simultaneously in both directions, the elements of $\Pi(n,:,:)$ must satisfy:

$$\pi_{\mathsf{orig},\mathsf{des}}(n)\pi_{\mathsf{des},\mathsf{orig}}(n) = 0, \ \forall\ n, \ \forall\ \mathsf{orig} \neq \mathsf{des}. \tag{18}$$

In addition, the elements of $\mathbf{\Pi}$ are all non-negative. We can interpret the diagonal elements of the matrix $\Pi(n,:,:)$ as the renewable power that the mth household transfers to itself, or, in other words, uses locally. Hence, we can let $\pi_{m,m}(n) = d_m(n)\ \forall\ m, \ \forall\ n$.

5.2. Transfer Charges

To ensure generality in our model, any grid-enabled energy transference can be subject to a charge. The utility bears the power loss resulting from the operation, and hence, it can impose a transfer fee on the users. To ensure generality, we consider transfer fees ranging from 0 to $[p_{\mathsf{des}}(n) - p_{\mathsf{orig}}(n)]$, where $p_{\mathsf{des}}(n)$ and $p_{\mathsf{orig}}(n)$ denote the prices at the destination and the origin, with $\mathsf{des},\ \mathsf{orig}\ \in \{1, \ldots, M\}$.[8] Therefore, the cost incurred by the set of households in moving $\Delta t \sum_{n=1}^{N} \sum_{m=1}^{M} \theta_m(n)$ energy units across the network is

$$\epsilon = \phi \Delta t \sum_{\mathsf{orig}=1}^{M} \sum_{\mathsf{des}=1}^{M} \sum_{n=1}^{N} \left[p_{\mathsf{des}}(n) - p_{\mathsf{orig}}(n) \right] \pi_{\mathsf{orig},\mathsf{des}}(n), \tag{19}$$

where $0 \leq \phi \leq 1$ is a parameter used to represent different pricing scenarios. If $\phi = 0$, then the transfer fee is zero, and the monetary value of the energy transferred from household orig to household des changes from $p_{\mathsf{orig}}(n)$ to $p_{\mathsf{des}}(n)$. On the other hand, if $\phi = 1$, then the transfer fee is $p_{\mathsf{des}}(n) - p_{\mathsf{orig}}(n)$, and hence, given the battery inefficiencies, transferring energy is not cost-effective. Between these two extremes there is an infinite range of possibilities, which are all captured by the model proposed.

5.3. Problem Formulation

With the considerations explained in Secs. 5.1 and 5.2, the optimization problem can be cast as follows:

$$\begin{aligned} \text{P1A:} \quad & \min_{\boldsymbol{c_1}, \ldots, \boldsymbol{c_M}, \, \boldsymbol{\Pi}} \ \chi + \epsilon \\ \text{s.t.} \quad & (1),\ (3),\ (7),\ (9),\ (11),\ \text{and } (18), \end{aligned} \tag{20}$$

where ϵ was defined in (19). In P1A, the objective function is the energy cost incurred by the entire group of households (χ), plus the cost incurred due to renewable energy transfers among its members. Quantities $\boldsymbol{j}_m$'s and $\boldsymbol{\Pi}$ are

[8] No energy transfer will take place if it costs more than buying the same amount of energy at the destination.

connected through (5). Quantities $\gamma_m(n)$ and $\theta_m(n)$ are defined in terms of $\mathbf{\Pi}$ in (2).

P1A is not a convex optimization problem because (18) states that there are sets of decision variables whose product must be zero at all times. Such equality constraints are not affine, and hence, P1A is not a convex optimization problem [58]. We can then find an alternative formulation, which we can later relax to a linear programming problem, and use in combination with other optimization techniques to find the optimal solution. We can thus cast the problem directly in terms of the $\boldsymbol{c}_m$'s, the $\boldsymbol{d}_m$'s, the $\boldsymbol{\theta}_m$'s, and the $\boldsymbol{\gamma}_m$'s as follows:

$$\begin{aligned} \text{P1B:} \quad & \min_{\boldsymbol{c_m},\, \boldsymbol{d_m},\, \boldsymbol{\theta_m},\, \boldsymbol{\gamma_m},\ m \,\in\, \{1,\ldots,M\}} \quad \chi + \epsilon \\ \text{s.t.} \quad & (1),\ (3),\ (7),\ (9),\ \text{and } (11). \end{aligned} \tag{21}$$

As defined in Eq. (19), ϵ is a function of the tensor $\mathbf{\Pi}$. Hence, to solve P1B, we write ϵ in terms of the $\boldsymbol{\theta}_m$'s and $\boldsymbol{\gamma}_m$'s, which can be done by noting the following:

$$\begin{aligned} \sum_{\mathsf{orig}=1}^{M} \sum_{\mathsf{des}=1}^{M} \sum_{n=1}^{N} \left[p_{\mathsf{des}}(n) - p_{\mathsf{orig}}(n)\right] \pi_{\mathsf{orig},\mathsf{des}}(n) = & \sum_{\mathsf{des}=1}^{M} \sum_{n=1}^{N} p_{\mathsf{des}}(n) \sum_{\mathsf{orig}=1}^{M} \pi_{\mathsf{orig},\mathsf{des}}(n) \\ & - \sum_{\mathsf{orig}=1}^{M} \sum_{n=1}^{N} p_{\mathsf{orig}}(n) \sum_{\mathsf{des}=1}^{M} \pi_{\mathsf{orig},\mathsf{des}}(n). \end{aligned} \tag{22}$$

Moreover, since $\gamma_{\mathsf{des}}(n) = \sum_{\mathsf{orig}=1}^{M} \pi_{\mathsf{orig},\mathsf{des}}(n)$ and $\theta_{\mathsf{orig}}(n) = \sum_{\mathsf{des}=1}^{M} \pi_{\mathsf{orig},\mathsf{des}}(n)$, ϵ can be written in terms of the $\gamma_{\mathsf{des}}(n)$'s and $\theta_{\mathsf{orig}}(n)$'s as follows:

$$\epsilon = \phi \Delta t \sum_{\mathsf{des}=1}^{M} \sum_{n=1}^{N} p_{\mathsf{des}}(n) \gamma_{\mathsf{des}}(n) - \sum_{\mathsf{orig}=1}^{M} \sum_{n=1}^{N} p_{\mathsf{orig}}(n) \theta_{\mathsf{orig}}(n), \tag{23}$$

The tensor $\mathbf{\Pi}$ can be determined from P1B's solution by using algorithms to solve non-negative least squares problems [59]. A detailed discussion on this procedure is presented in Appendix 9.

5.4. Solution Strategy

Our approach to solve problem P1B is to introduce a matrix formulation and to relax constraint (3). Specifically, in order to cast P1B in standard linear

programming form, (3) is relaxed to an inequality-type constraint. To solve P1B we introduce the following definition:

$$\mathbf{G}_m = [\alpha_m \Delta t \mathbf{A}_N \quad -\frac{1}{\beta_m}\Delta t \mathbf{A}_N \quad -\frac{1}{\beta_m}\Delta t \mathbf{A}_N \quad \mathbf{0}_{N,N}], \tag{24}$$

where $\mathbf{A}_N$ is the $N \times N$ lower triangular matrix of ones. Clearly, $\mathbf{G}_m$ is an $N \times 4N$ matrix. By using $\mathbf{G}_m$, constraint (7) can be rewritten compactly as follows:

$$\mathbf{0}_{N,1} \preceq \mathbf{G}_m \begin{pmatrix} \mathbf{c}_m \\ \mathbf{d}_m \\ \boldsymbol{\theta}_m \\ \boldsymbol{\gamma}_m \end{pmatrix} \preceq [\Psi_m - j_m(0)]\, \mathbf{1}_{N,1},\ \forall\ m. \tag{25}$$

Let $\mathbf{v}_1 = [(\Psi_1 - j_1(0))\mathbf{1}_{1,N}, \ldots, (\Psi_M - j_M(0))\mathbf{1}_{1,N},\ \mathbf{0}_{1,NM}]$ and $\mathbf{v}_2 = [q_D \mathbf{1}_{1,NM}, \mathbf{0}_{1,N}]$. Then, the constraints in P1B can be written as $\mathbf{Be} \preceq \mathbf{f}$, where

$$\mathbf{B} = \begin{pmatrix} \mathbf{I}_M \otimes \mathbf{G}_m \\ -\mathbf{I}_M \otimes \mathbf{G}_m \\ \mathbf{I}_M \otimes [\mathbf{I}_N \ \ \mathbf{0}_{N,2N} \ \ -\mathbf{I}_N] \\ \mathbf{I}_M \otimes [\mathbf{0}_{N,N} \ \ \mathbf{I}_N \ \ \mathbf{I}_N \ \ \mathbf{0}_{N,N}] \\ \mathbf{1}_{1,M} \otimes [\mathbf{0}_{N,2N} \ \ -\mathbf{I}_N \ \ \mathbf{I}_N] \end{pmatrix},\ \mathbf{e} = \begin{pmatrix} \mathbf{c}_1 \\ \mathbf{d}_1 \\ \boldsymbol{\theta}_1 \\ \boldsymbol{\gamma}_1 \\ \vdots \\ \mathbf{c}_M \\ \mathbf{d}_M \\ \boldsymbol{\theta}_M \\ \boldsymbol{\gamma}_M \end{pmatrix}, \tag{26}$$

and $\mathbf{f} = [\mathbf{v}_1, \mathbf{r}_1^T, \ldots, \mathbf{r}_M^T, \mathbf{v}_2]^T$. As seen, $\mathbf{e} \in \mathbb{R}_+^{4MN}$, $\mathbf{B} \in \mathbb{R}^{(4MN+N)\times(4MN)}$, and $\mathbf{f} \in \mathbb{R}_+^{4MN+N}$. If we relax (3) to

$$\sum_{m=1}^{M} \gamma_m(n) \leq \sum_{m=1}^{M} \theta_m(n),\ \forall\ n, \tag{27}$$

then, the optimization problem P1B can be cast as a linear program by using the definitions given above. Introducing this relaxation does not affect the solution

because a necessary[9] condition for optimality is that the $\boldsymbol{\gamma}_m$'s and the $\boldsymbol{\theta}_m$'s must satisfy (27) with equality. Therefore, constraint (3) will be automatically satisfied by the solution simply by enforcing its relaxed version in (27).

6. Comparative Analysis

This section is divided in three parts. In the first part we introduce two alternative performance criteria, which aim at quantifying the renewable energy utilization rate in each of the studied configurations. In the second part we outline the main differences between the two configurations. In the third part we show how the proposed framework can be used to devise real-time renewable energy management algorithms by incorporating forecasting of renewable energy production and load.

6.1. Alternative Performance Criteria

The proposed strategies can be compared in terms of the achievable cost savings and the renewable energy remaining unused due to battery limitations. In the following we quantify the renewable energy left unused in each strategy. Renewable energy is left unused when the power delivered by the generator is above the maximum charging rate allowed, or, when the batteries are fully charged. Let $\boldsymbol{d_1}^*, \ldots, \boldsymbol{d_M}^*$ and $\tilde{\boldsymbol{d}}_{\boldsymbol{1}}^{\,*}, \ldots, \tilde{\boldsymbol{d}}_{\boldsymbol{M}}^{\,*}$ denote the optimal discharging profiles obtained by solving P0 and P1B respectively. Then, the renewable energy left unused in the configuration with CREG is

$$\mathsf{REU}_C = \Delta t \sum_{n=1}^{N} \left[r(n) - \sum_{m=1}^{M} d_m^*(n) \right]. \tag{28}$$

Similarly, the renewable energy left unused in the configuration with DREG is

$$\mathsf{REU}_D = \Delta t \sum_{m=1}^{M} \sum_{n=1}^{N} \left[r_m(n) - \tilde{d}_m^*(n) \right]. \tag{29}$$

[9]This can be proved by contradiction. An intuitive explanation is the following: A necessary condition for optimality is to minimize energy waste. Therefore, the energy transfer process should be such that, ignoring losses, the total energy drawn from the sourcing households must be equal to the total energy received by the destination households.

By the principle of conservation of energy we must have $\mathsf{REU}_C \geq 0$ and $\mathsf{REU}_D \geq 0$. The proposed strategies can be compared to a baseline scheme in which no optimization is performed, i.e., the renewable energy is used while it is being generated. In the baseline strategy the excess renewable energy is discarded and no storage device is needed. The households in the configuration with DREG can opt for using a greedy strategy, in which they selfishly minimize their own energy expenditure, without sharing renewable energy with others. In the greedy approach, each household solves the following problem to minimize its own energy cost:

$$\begin{aligned} \text{P2:} \quad & \min_{\boldsymbol{c_m},\, \boldsymbol{d_m},\, m \,\in\, \{1,\ldots,M\}} \quad \xi_m \\ \text{s.t.} \quad & (1),\ (7),\ (9),\ (11) \end{aligned} \tag{30}$$

and $\theta_m(n) = 0,\ \gamma_m(n) = 0,\ \forall\ m,\ \forall\ n$. As seen, P2 is a special case of P1A, and hence, it can be solved by using the strategy proposed in Sec. 5.4.

6.2. CREG vs. DREG

Given their distinct characteristics, the strategies proposed in Secs. 4 and 5 will have different performance. To establish a baseline for comparison purposes, we first derive the conditions under which both strategies achieve the same performance.

The strategies proposed in Secs. 4 and 5 will achieve the same performance if the following conditions are satisfied:

- Zero power transfer fees are enforced in the configuration with DREG, i.e. $\phi = 0$. As a result, renewable energy can be allocated across households at no cost in both configurations.

- Both configurations offer the same level of energy management flexibility when the charging/discharging rates are such that:

$$q_{C,m} \geq \max\left\{ \frac{\sum_{m=1}^{M} \Psi_m}{\Delta t}, \sum_{m=1}^{M} r_m(n) \right\},\ \forall\ m,\ \forall\ n. \tag{31}$$

$$q_{D,m} \geq \max\left\{\frac{\sum_{m=1}^{M}\Psi_m}{\Delta t}, \sum_{m=1}^{M}\ell_m(n)\right\},\ \forall\ m,\ \forall\ n. \tag{32}$$

$$q_C \geq \max\left\{\frac{\Psi}{\Delta t}, \sum_{m=1}^{M} r_m(n)\right\},\ \forall\ n, \tag{33}$$

$$q_D \geq \max\left\{\frac{\Psi}{\Delta t}, \sum_{m=1}^{M}\ell_m(n)\right\},\ \forall\ n. \tag{34}$$

Conditions (31) and (33) allow full battery charging within a single time slot, and enable zero renewable energy waste. Similarly, (32) and (34) allow full battery depletion within a single time slot, and enable full load serving in all time slots.

- Both configurations incur the same power loss:

$$(1-\alpha)\sum_{n=1}^{N} c^*(n) = \sum_{m=1}^{M}(1-\alpha_m)\sum_{n=1}^{N} c_m^*(n). \tag{35}$$

$$\frac{1-\beta}{\beta}\sum_{n=1}^{N}\sum_{m=1}^{M} d_m^*(n) = \sum_{m=1}^{M}\frac{1-\beta_m}{\beta_m}\sum_{n=1}^{N}\left[\pi_{m,m}^*(n)+\theta_m^*(n)\right]. \tag{36}$$

Condition (35) states that the energy losses incurred in the charging operations are the same in both CREG and DREG configurations. Condition (36) states that the energy losses incurred in the discharging operations are the same in both CREG and DREG configurations.

- Both configurations have the same energy storage capacity:

$$\Psi = \sum_{m=1}^{M}\Psi_m. \tag{37}$$

- The renewable energy left unused is the same in both configurations:

$$\sum_{n=1}^{N}[r(n)-c^*(n)] = \sum_{m=1}^{M}\sum_{n=1}^{N}[r_m(n)-c_m^*(n)]. \tag{38}$$

If $\alpha_m = \alpha,\ \forall\ m$, then (38) reduces to $\sum_{n=1}^{N} r(n) = \sum_{m=1}^{M}\sum_{n=1}^{N} r_m(n)$. Similarly, if $\beta_m = \beta_j,\ \forall\ m,\ j$, and

$$\sum_{n=1}^{N}\sum_{m=1}^{M} d_m^*(n) = \sum_{m=1}^{M}\sum_{n=1}^{N}\left[\pi_{m,m}^*(n)+\theta_m^*(n)\right], \tag{39}$$

then (36) reduces to $\beta_m = \beta,\ \forall\ m$. This is thus a particular set of requirements which suffice to satisfy (35), (36), and (38).

Finally, we list the following structural differences between CREG and DREG:

- Geographical diversity: The location of the renewable energy generators has an impact on the statistical variability of the total renewable energy generation in each configuration, which in turn, will lead to performance differences. This issue is discussed in Sec. 8.

- Storage devices: The configuration with CREG requires larger batteries and higher discharging rates. Such devices may be more expensive than the storage devices used in the configuration with DREG, which can be smaller. However, the configuration with CREG offers a higher level of flexibility because *only* the total power charged or discharged is constrained. Contrarily, in the configuration with DREG, each charging/discharging operation is constrained by the limitations of the local storage device.

- Capital cost: In the configuration with CREG, power lines connecting the households and the energy farm need to be deployed. Contrarily, the configuration with DREG uses the grid as a means for cooperation among the participants. This distinction raises the question how energy transfer fees and energy farm investment impact the choice of configuration. This problem will be investigated in future works.

7. Real-time renewable energy Management Algorithm

7.1. Real-Time renewable energy Management

In this section we show how the proposed framework can be used to devise real-time renewable energy management algorithms. We denote the estimates of $\mathbf{r}_m$, $\mathbf{r}$ and $\boldsymbol{\ell}_m$ by using $\hat{\mathbf{r}}_m$, $\hat{\mathbf{r}}$, and $\hat{\boldsymbol{\ell}}_m$, respectively.[10] The proposed real-

[10]The forecasts $\hat{\mathbf{r}}$, $\hat{\mathbf{r}}_m$, and $\hat{\boldsymbol{\ell}}_m$ can be determined by using techniques based on time series analysis, weather forecasts, or machine learning methods.

time renewable energy management strategy, applied to the configuration with centralized renewable energy generation, is shown in Algorithm 1. Similarly, the real-time renewable energy management strategy proposed for the configuration with distributed renewable energy generation is shown in Algorithm 2.

As observed in Algorithms 1 and 2, we use the framework developed in Secs. 4 and 5 to update the decision variables in response to new measurements and estimates. As seen, forecasting techniques are used to estimate future renewable energy generation and load. To improve the accuracy of the estimations, the statistical models of energy generation and load can be updated as new measurements are recorded. Moreover, the frequency at which the decision variables are updated can be decreased to reduce the computational complexity of the proposed algorithms. This can be implemented by conditioning the update to deviations between the observations and the forecasts, in which case a new instance of the optimization problem is solved only when the forecasts significantly deviate from the observations.

Algorithm 1 Forecasting-based real-time renewable energy management algorithm, configuration with centralized renewable energy generation

1: Estimate parameters of statistical models of $\mathbf{r}$ and $\boldsymbol{\ell}_m,\ m \in \{1, \ldots, M\}$.
2: Initialize the estimates $\hat{\mathbf{r}}$ and $\hat{\boldsymbol{\ell}}_m$.
3: Solve optimization problem by using $\hat{\mathbf{r}}$ and $\hat{\boldsymbol{\ell}}_m$. Determine the $d_m(1)$'s.
4: Estimate $j(1)$.
5: **for** $n = 2$ **to** N **do**
6: Measure $r(n)$ and $\ell_m(n)$.
7: Update $\hat{\mathbf{r}}$ and $\hat{\boldsymbol{\ell}}_m$.
8: Solve the optimization problem (P0) by using updated estimates and recorded observations (measurements).
9: Update estimate of $\mathbf{j}$: $j(n) = j(n-1) + \Delta t \left[\alpha c(n) - \frac{1}{\beta} \sum_{m=1}^{M} d_m(n)\right]$.
10: Adjust the $d_m(n)$'s if $j(n) > \Psi$ or $j(n) < 0$.
11: **end for**

Algorithm 2 Forecasting-based real-time renewable energy management algorithm, configuration with distributed renewable energy generation

1: Estimate parameters of the statistical models of $\mathbf{r}_m$ and $\boldsymbol{\ell}_m$, $m \in \{1, \ldots, M\}$.
2: Initialize the estimates $\hat{\mathbf{r}}_m$ and $\hat{\boldsymbol{\ell}}_m$.
3: Solve optimization problem by using $\hat{\mathbf{r}}_m$ and $\hat{\boldsymbol{\ell}}_m$. Determine the $d_m(1)$'s, the $\theta_m(1)$'s and the $\gamma_m(1)$'s.
4: Estimate the $j_m(1)$'s.
5: **for** $n = 2$ **to** N **do**
6: Measure $r_m(n)$ and $\ell_m(n)$.
7: Update $\hat{\mathbf{r}}_m$ and $\hat{\boldsymbol{\ell}}_m$.
8: Solve the optimization problem (P1B) by using updated estimates and recorded observations (measurements).
9: Update estimate of $\mathbf{j}_m$: $j_m(n) = j_m(n-1) + \Delta t \alpha_m c_m(n) - \frac{1}{\beta_m}[d_m(n) + \theta_m(n)]$.
10: Adjust the $d_m(n)$'s if $j_m(n) > \Psi_m$ or $j_m(n) < 0$.
11: **end for**

The proposed algorithms approach the genie-aided solution when the estimates $\hat{\mathbf{r}}$, $\hat{\mathbf{r}}_m$, and $\hat{\boldsymbol{\ell}}_m$ are close to the actual renewable energy generation and load profiles. To complete Step 8 in Algorithms 1 and 2, the optimization problem can be solved by restricting the time horizon to the period $[n\Delta t, T]$. Therefore, the time required to complete each of the $N-1$ executions of Step 8 decreases as n approaches N. The frequency at which the decision variables $\mathbf{d}_m$'s are updated can also be decreased to reduce the computational complexity of the algorithms. We can also reduce the rate at which the estimates $\hat{\mathbf{r}}$ and $\hat{\boldsymbol{\ell}}_m$ are updated in order to avoid invoking the forecasting algorithm in each of the $N-1$ executions.

8. Numerical Results

We provide simulation results to verify the analysis developed in the paper, and compare the performance of the proposed strategies. Unless otherwise stated, throughout this section we consider the simulation parameters shown in Table 2, where minPrice, maxPrice, minLoad, maxLoad, minGen, and maxGen are all real numbers chosen to study different simulation scenarios. The uniform distribution is chosen for the prices, the renewable energy generation, and the load, because it reflects total uncertainty about a random quantity given that we know its lower and upper limit.[11] The optimization problems are solved by using Scilab's `linpro()` function. The results shown in this section are obtained by averaging over ten thousand realizations. Storage capacity is measured in energy units [EU] and energy expenditure in monetary units [MU].

8.1. Sensitivity to renewable energy Distribution

We consider the simulation scenario shown in Table 2, except for $r(n)$, which we choose uniformly distributed between minGen, and MmaxGen. Other parameters are set as follows minLoad $= 1$, maxLoad $= 1$, minGen $= 0$, maxGen $= 2$,

[11] In practice, prices, loads and renewable energy generation are all upper bounded, moreover, their natural lower bound is 0.

Table 2: Simulation Scenarios

Parameter	**Value/Property**
$\{N,\ \Delta t,\ M,\ \phi\}$	$\{24,\ 1,\ 2,\ 0,\ \forall\ m\}$
$p_m(n)$	$\sim \mathcal{U}(\mathsf{minPrice}, \mathsf{maxPrice})$
$\ell_m(n)$	$\sim \mathcal{U}(\mathsf{minLoad}, \mathsf{maxLoad})$
$r_m(n)$	$\begin{cases} \sim \mathcal{U}(\mathsf{minGen}, \mathsf{maxGen}), & n \in \{1, \lceil N/2 \rceil\} \\ 0 & n > \lceil N/2 \rceil \end{cases}$
$r(n)$	$\sum_{m=1}^{M} r_m(n)$
q_C	$\max\left\{\frac{\Psi}{\Delta t}, M\mathsf{maxGen}\right\}$
q_D	$\max\left\{\frac{\Psi}{\Delta t}, M\mathsf{maxLoad}\right\}$
$q_{C,m}$	$\max\left\{M\frac{\Psi_m}{\Delta t}, M\mathsf{maxGen}\right\}$
$q_{D,m}$	$\max\left\{M\frac{\Psi_m}{\Delta t}, M\mathsf{maxLoad}\right\}$
$\Psi_m,\ j_m(0)$	$\Psi_1,\ 0,\ \forall\ m$
$\{\alpha,\ \beta,\ \Psi,\ j(0)\}$	$\{1,\ 1,\ M\Psi_m,\ 0\}$

$\mathsf{minPrice} = 0$, $\mathsf{maxPrice} = 1$. Then, in Fig. 2 we plot the average energy cost incurred in the N-slot planning period, and the average amount of renewable energy unused, both against the storage size Ψ_m, which ranges from 1 to 10 [EU]. As observed, in this scenario, DREG outperforms CREG. This follows because the variability in the renewable energy generation is different in each configuration. In the configuration with DREG, the independence of the random variables $r_1(n)$ and $r_2(n)$ models geographical diversity. Although the average renewable energy generation is the same in both configurations, the variance of $r(n)$ is larger than the variance of $r_1(n) + r_2(n)$. The gap between the two results is small because other simulation parameters have been chosen to comply with the conditions explained in Sec. 6.2. Hence, these tests are only meant to evaluate the impact of the statistical distribution of the renewable energy generation in both configurations. It is also observed that the gap between the two configurations decreases as the storage capacity increases, which may be due to a reduced amount of renewable energy left unused when $\Psi_m > 6$ [EU].

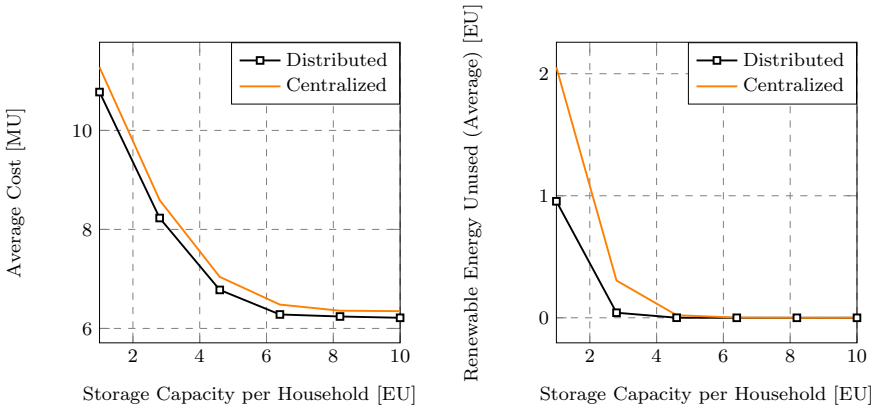

Figure 2: Energy cost vs. storage capacity per household. Distributed renewable energy generation outperforms centralized renewable energy generation due to geographical diversity.

8.2. Sensitivity to Charging/Discharging Rates

We consider the simulation scenario shown in Table 2, except for $q_{C,m}$, $q_{D,m}$, q_C and q_D, which we set as follows: $q_{C,m} = 0.2\frac{\Psi_m}{\Delta t}$, $q_{D,m} = 0.2\frac{\Psi_m}{\Delta t}$, $q_C = 0.2\frac{\Psi_m}{\Delta t}$ and $q_D = 0.2\frac{\Psi_m}{\Delta t}$. Moreover, we let $\mathsf{minLoad} = 1$, $\mathsf{maxLoad} = 1$, $\mathsf{minGen} = 0$, $\mathsf{maxGen} = 2$, $\mathsf{minPrice} = 0$, and $\mathsf{maxPrice} = 1$. Then, in Fig. 3 we plot the average energy cost incurred in the N-slot planning period, and the average amount of renewable energy unused, both against the storage size Ψ_m, which ranges from 1 to 10 [EU]. As observed, in this scenario, DREG outperforms CREG because the maximum charging and discharging rates are higher in the configuration with DREG, since $q_{C,1} + q_{C,2} > q_C$ and $q_{D,1} + q_{D,2} > q_D$. As seen in Fig. 3, lower charging/discharging rates lead to lower usability of renewable energy, and smaller cost savings.

We now consider the simulation scenario shown in Table 2, except for $q_{C,m}$, $q_{D,m}$, q_C and q_D, which we set as follows: $q_{C,m} = 0.2\frac{\Psi_m}{\Delta t}$, $q_{D,m} = 0.2\frac{\Psi_m}{\Delta t}$, $q_C = 0.2M\frac{\Psi_m}{\Delta t}$ and $q_D = 0.2M\frac{\Psi_m}{\Delta t}$. Other parameters are set as follows: $\mathsf{minLoad} = 1$, $\mathsf{maxLoad} = 1$, $\mathsf{minGen} = 0$, $\mathsf{maxGen} = 2$, $\mathsf{minPrice} = 0$, and $\mathsf{maxPrice} = 1$. Then, in Fig. 4 we plot the average energy cost incurred in the planning period, and the average amount of renewable energy unused, both against the storage

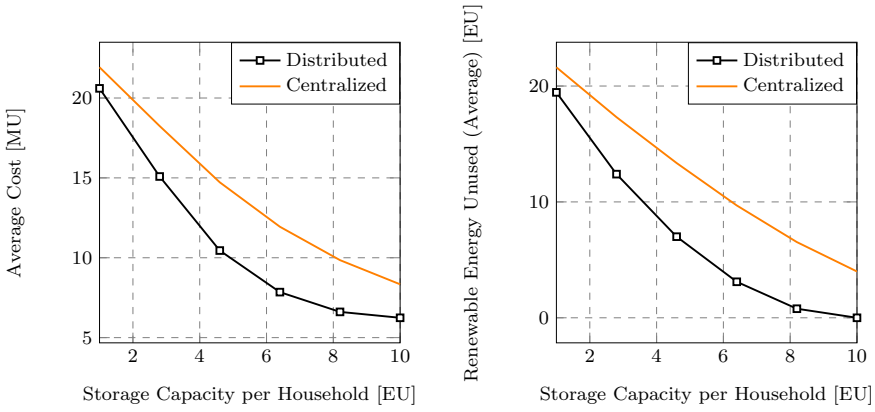

Figure 3: Energy cost vs. storage capacity. DREG outperforms CREG because in this scenario CREG has lower charging/discharging rates.

size Ψ_m, which ranges from 1 to 10 [EU]. As observed, in this scenario, the configuration with CREG outperforms the configuration with DREG. However, the gap between the two strategies reduces as the storage capacity increases. This result follows because the maximum charging and discharging rates are the same in both configurations, i.e. $q_{C,1} + q_{C,2} = q_C$ and $q_{D,1} + q_{D,2} = q_D$, and the configuration with CREG has a higher level of flexibility to move renewable energy to the location with the highest prices, while the configuration with DREG is constrained by the limit in the charging/discharging rates ($q_{C,m} = 0.2\frac{\Psi_m}{\Delta t}$, $q_{D,m} = 0.2\frac{\Psi_m}{\Delta t}$) which are, respectively, below the thresholds (31) and (32) established to ensure the same performance in both configurations.

8.3. Equal-Performance Scenarios

We reproduce the conditions described in Sec. 6.2 to verify that they lead to the same performance in both configurations. We consider the simulation parameters shown in Table 2 with $\mathsf{minLoad} = 1$, $\mathsf{maxLoad} = 1$, $\mathsf{minGen} = 0$, $\mathsf{maxGen} = \{1, 2\}$, $\mathsf{minPrice} = 0$, $\mathsf{maxPrice} = 1$, and plot the average results obtained after ten thousand realizations in Fig. 5. As shown in Fig. 5, the two strategies lead to similar results when the conditions stated in Sec. 6.2

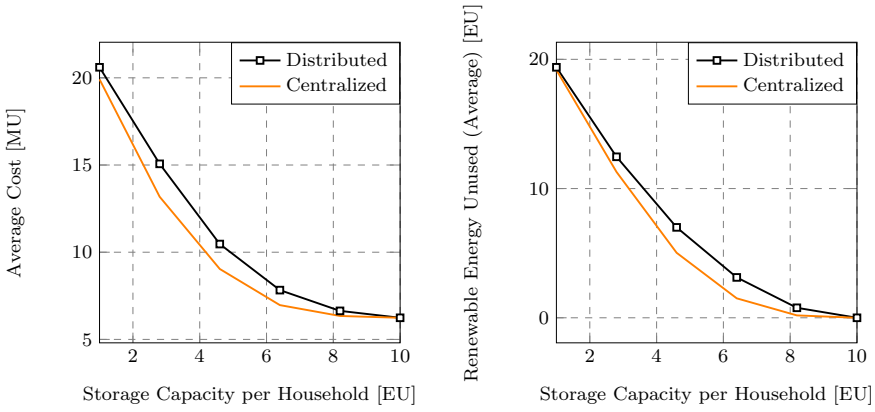

Figure 4: Energy cost vs. storage capacity. CREG outperforms DREG if it features higher charging/discharging rates.

Table 3: Unoptimized vs. Optimized Cost

maxGen	Unoptimized	Optimized, $\Psi = 1$	Optimized, $\Psi = 10$
1	18[MU]	14.6[MU]	13.6[MU]
2	12[MU]	10.7[MU]	6.2[MU]

are enforced. Table 3 shows the cost reduction achieved by using the proposed strategies in the same simulation scenarios. As seen, the proposed strategies are able to reduce the households' energy expenditure by up to 48%. The gap between the proposed strategies and the baseline strategy increases with the generation capacity (maxGen).

8.4. Cooperative vs. Greedy Approach

We compare the strategy proposed for households with DREG, and the greedy approach explained in Sec. 6.1. We consider the simulation scenario shown in Table 2, with minLoad $= 1$, maxLoad $= 1$, minGen $= 0$, maxGen $= \{1, 2\}$, minPrice $= 0$, maxPrice $= 1$, and in Fig. 6 we plot the average energy cost incurred, and the average amount of renewable energy unused, both against the storage size Ψ_m. As observed, the cooperative solution outperforms the greedy strategy, especially for small values of Ψ_m. Moreover, the greedy strategy leads

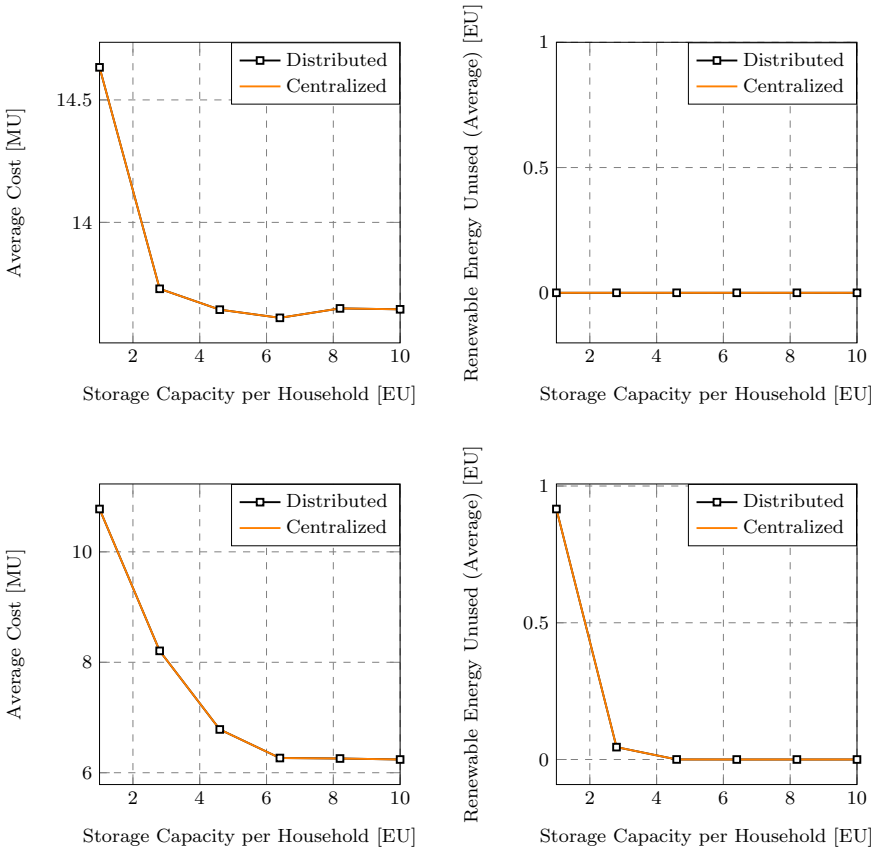

Figure 5: Energy cost vs. storage capacity. Both configurations achieve the same performance if conditions are satisfied. Top: $\mathsf{maxGen} = 1$, bottom: $\mathsf{maxGen} = 2$.

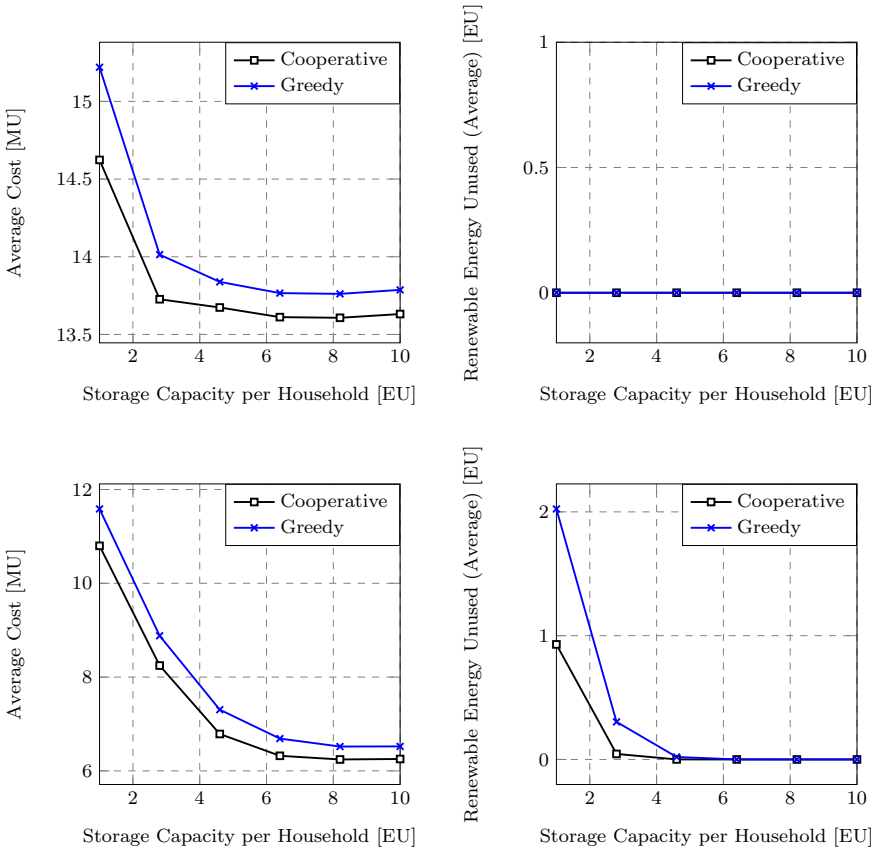

Figure 6: Energy cost vs. storage capacity per household. Cooperative strategy outperforms greedy approach. Top: maxGen = 1, bottom: maxGen = 2.

to a lower utilization of renewable energy, especially when the storage capacity is small. If the generation capacity increases, i.e. if maxGen = 2, then the amount of renewable energy remaining unused is larger in the greedy approach, especially when the storage capacity is below 4 [EU].

8.5. Real-time renewable energy Management Algorithm

We consider the simulation parameters shown in Table 2, except for $r(n)$, which we set as

$$r(n) = \begin{cases} \sim \mathcal{U}(\mathsf{minGen}, M\mathsf{maxGen}), & n \in \{1, \lceil N/2 \rceil\} \\ 0 & n > \lceil N/2 \rceil \end{cases}. \tag{40}$$

The rest of parameters are set as $\mathsf{minGen} = \mathsf{minLoad} = \mathsf{minPrice} = 0$, $\mathsf{maxPrice} = 1$, $\mathsf{maxGen} \in \{1, 2\}$, and $\mathsf{maxLoad} \in \{1, 2\}$.

To show the robustness of the proposed algorithms we choose a simple stochastic model for the renewable energy generation and power consumption. The chosen statistical model is simple and disregards the intertemporal correlation in $\mathbf{r}$ and $\boldsymbol{\ell}$. As a result, the forecasting errors will be large, but suitable to show the robustness of the algorithm. Given the statistical model considered for $\mathbf{r}$ and $\boldsymbol{\ell}_m$, the best estimates that we can use are

$$\hat{r}(n) = \frac{\mathsf{minGen} + \mathsf{maxGen}}{2} \tag{41}$$

and

$$\hat{\ell}_m(n) = \frac{\mathsf{minLoad} + \mathsf{maxLoad}}{2}, \ \forall \ m, \tag{42}$$

which are meant to minimize the mean-squared error.

We average over the results of ten thousand experiments and obtain the plots of Fig. 7. As seen, there is a performance gap between the real-time algorithm and the genie aided strategy. The gap grows with the variance of $\mathbf{r}$ and $\boldsymbol{\ell}_m$, which, leads to larger forecasting errors. This gap can be reduced by using more accurate forecasts.

Although the forecasting errors can be as high as 50% of the maximum renewable energy generation or power consumption, the worst observed performance gap corresponds to only 15% of the optimized cost. This demonstrates the ability of the proposed real-time algorithms to handle uncertainty. It is important to highlight that the genie aided strategy is an essential part of our real-time algorithms, and which ultimately allows us to evaluate its performance by establishing the corresponding benchmark.

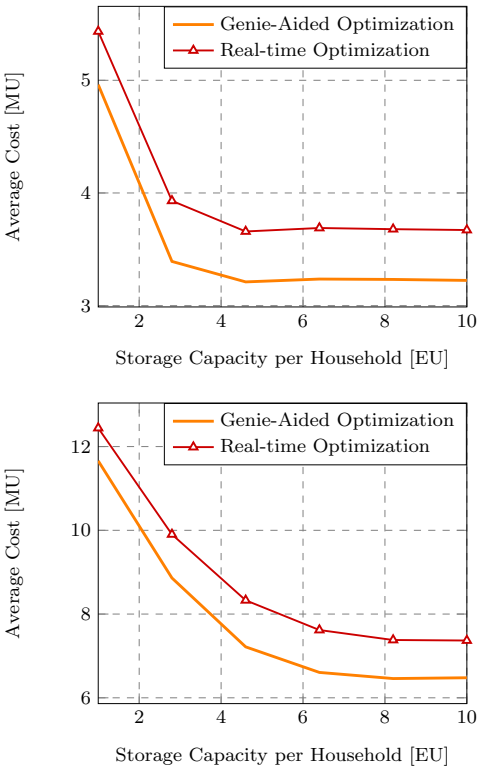

Figure 7: Performance of Algorithm 1. Top: maxGen = maxLoad = 1. Bottom: maxGen = maxLoad = 2.

Table 4: Simulation Setup Real Time Energy Management.

Feature	**Approach**	
	Stochastic programming	**Forecasting-based**
Energy generation model	$r_1(n) \sim \mathcal{N}(\rho_1(n), \sigma^2),\ \forall\ n$ $r_2(n) \sim \mathcal{N}(\rho_2(n), \sigma^2),\ \forall\ n$	
Estimated energy generation	$\hat{r}_1(n) = \rho_1(n),\ \forall\ n$ $\hat{r}_2(n) = \rho_2(n),\ \forall\ n$	
Errors due to:	Inaccurate identification	Inaccurate forecasting

8.6. Comparison with Existing Works

We now compare the proposed real-time renewable energy management algorithms with existing strategies. Works such as [41, 42, 47] use stochastic programming techniques to optimize the average energy cost incurred by renewable energy systems. Since most of the existing strategies are designed for non-cooperative households, we restrict our simulations to scenarios with a single household, i.e., in this section we consider $M = 1$.

Existing strategies such as the ones presented in [41, 42, 47] aim at optimizing the average energy cost incurred by the system. The performance of such strategies depends on the accuracy of the statistical model employed. Similarly, the performance of the proposed strategies depend on the forecasting errors. The considerations undertaken to perform such a comparison are summarized in Table 4 and explained in more detail as follows:

- Stochastic model: We consider two average renewable energy generation profiles $\boldsymbol{\rho}_1 \in \mathbb{R}^N$ and $\boldsymbol{\rho}_2 \in \mathbb{R}^N$, each with a 50% probability of occurrence. The actual renewable energy generation will follow a Gaussian random process whose mean could be either $\boldsymbol{\rho}_1$ or $\boldsymbol{\rho}_2$, and whose standard deviation is σ.

- In the approach based on stochastic programming, performance degradation is incurred after wrongly identifying the average renewable energy

generation profile. The probability of identifying the correct renewable energy generation profile is denoted by δ and satisfies $\delta < 1$.

- In the forecasting-based algorithm, performance degradation is incurred as a result of forecasting errors. Specifically, the point forecasts are given by the mean value of the process, i.e., the chosen estimation performance measure is the mean-squared error. Hence, the forecasting error will be proportional to the variance of the Gaussian process.

With the considerations described above and summarized in Table 4, we employ the following simulation scenario: $\rho_1(n) = 5\cos\left(\frac{\pi}{12}(n-12)\right) + 5$, $\rho_2(n) = 1.5\cos\left(\frac{\pi}{12}(n-12)\right)+1.5$, $\sigma = 0.1$, $p_1(n) = \sin\left(\frac{\pi}{12}(n-12)\right)+1$, $N = 24$, $\Delta t = 1$, and the battery parameters listed in Table 2. Then, we compare the proposed forecasting-based approach with the existing strategies based on stochastic programming. Ten thousand experiments are run and the results are shown in Fig. 8, where we have plotted the average cost savings against energy storage capacity per household. It is seen that the proposed real-time algorithms outperform the existing approach by up to 10%. As expected, this performance gap grows as the value of δ increases. The proposed algorithms outperform existing strategies because they allow us to leverage correlations in the renewable energy generation process across time, so as to enhance the accuracy of the predictions. It also responds to observations in real time by adjusting the statistical model, the forecasts, and the decision variables.

8.7. Practical Case Study

We now use realistic system parameters to evaluate the optimization framework in a practical scenario. We consider the time-varying electricity prices offered by Southern California Edison to its medium size customers on a hot summer day [60]. We also consider the typical renewable energy generation profile of a solar panel with characteristics listed in Table 5, which was computed by using the PVWatts calculator provided by the National Renewable Energy Lab [61]. Furthermore, we consider the average power consumption profile of a

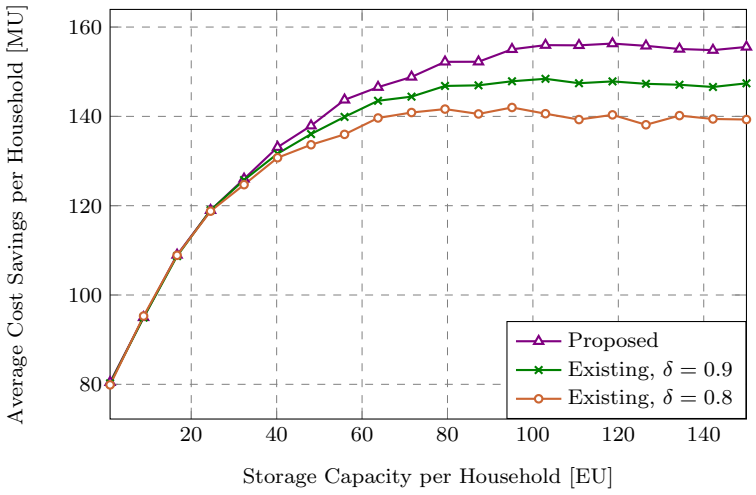

Figure 8: The proposed real-time energy management algorithms outperform the existing approach. The performance gap is larger for smaller δ.

Table 5: Photovoltaic system (Southern California)

Latitude, Longitude	**System size**	**Tilt, Azimuth**	**Inverter efficiency**	**DC to AC size ratio**	**Losses**
32.7° N, 117.2° W	4 kW (DC)	20°, 180°	96%	1.2	14%

household in September, which we denote by $\bar{\boldsymbol{\ell}}$, and was taken from [62], where authors develop techniques to estimate the hourly electricity consumption of Japanese households. The overall characteristics of the simulation scenario are presented in Table 6 and in Fig. 9, where we also illustrate the optimal renewable energy consumption schedule for the plotted power consumption profiles. Both, CREG and DREG configurations are considered under the conditions for even performance explained in Sec. 6.2.

We implemented the simulation scenario described in Table 6 with the battery parameters listed in Table 2, with $\Psi_1 = \Delta t \sum_{n=1}^{N} r(n)$, and the pricing and renewable energy generation profiles plotted in Fig. 9. The average cost in-

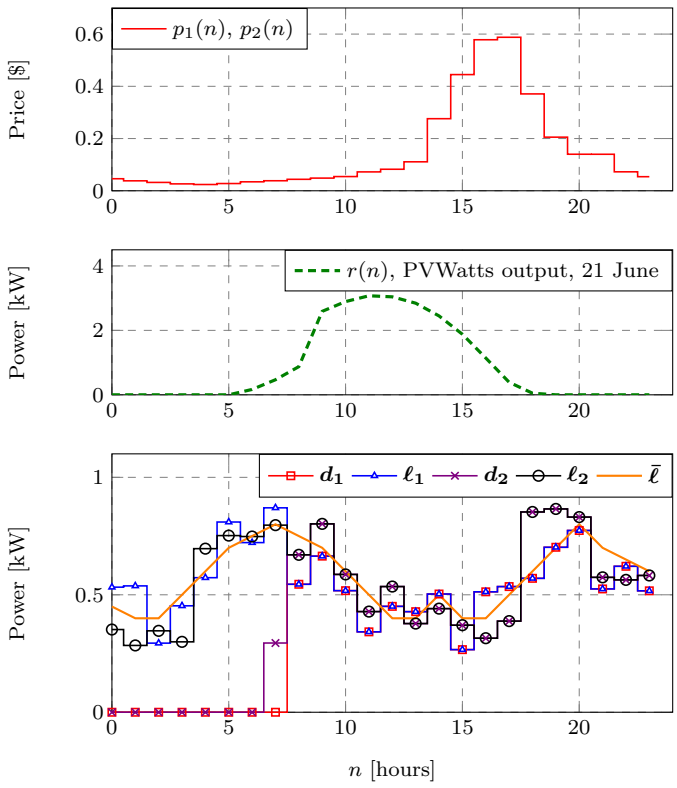

Figure 9: Practical case. The optimal renewable energy consumption schedules are plotted for the shown realizations of the power consumption profile.

Table 6: Simulation Scenario Practical Case

Parameter	**Value/Property**
$\{N,\ \Delta t,\ M,\ \phi\}$	$\{24,\ 1,\ 2,\ 0,\ \forall\ m\}$
$\ell_m(n)$	$\sim \mathcal{N}\left(\bar{\ell}(n), \sigma^2\right),\ \forall\ m$ and $\mathbb{E}\left[\ell_1(n)\ell_2(n)\right] = 0,\ \forall\ n$

curred when using the proposed optimization framework is \$0.3. The average cost incurred without any[12] optimization was \$1.9.

9. Conclusions

We have proposed cooperation methods with different energy production and storage configurations. In the first configuration, a group of households share access to an energy farm, whereas in the second configuration, each household is equipped with its own energy generator and storage device. We have then proposed strategies to minimize the energy expenditure incurred by the participating households in each configuration. The proposed strategies account for location- and time-varying energy prices, and have been obtained by solving constrained optimization problems through a combination of techniques.

Simulation results have demonstrated that the proposed strategies can lead to significant cost savings in both configurations. Moreover, we have established the conditions under which the two configurations lead to the same results, and shown that the best performing configuration is the one with the highest energy management flexibility. Similarly, through simulations we have shown that, in the configuration with distributed generation, the proposed cooperative strategy outperforms the greedy approach, especially when the energy storage capacity is limited.

[12] When no optimization is performed, the available renewable energy is evenly allocated across households. Excess renewable energy generation is discarded.

We have also proposed real-time renewable energy management strategies based on forecasting techniques. These strategies are based on a continuous re-computation of the decision variables, whose update rate can be adjusted in accordance with the available computational resources. Simulations have been used to show that the proposed algorithms outperform the existing approach and are robust to forecasting errors.

Appendix A: Power Transfer Tensor from P1B's Solution

By solving the alternative problem P1B, we seek to optimize the quantities $\boldsymbol{\theta}_m$, $\boldsymbol{\gamma}_m$, and $\boldsymbol{d}_m$. Consequently, we claim that the power transfer tensor can be determined from the optimized $\boldsymbol{\theta}_m$, $\boldsymbol{\gamma}_m$, and $\boldsymbol{d}_m$, thus solving the original P1A. In the following we explain the procedure to determine the power transfer tensor from the vectors $\boldsymbol{\theta}_m$, $\boldsymbol{\gamma}_m$, and $\boldsymbol{d}_m$.

First, we note that the diagonal elements of the matrix $\Pi(n,:,:)$ are optimized directly, they indeed correspond to the $\mathbf{d}_m$'s, i.e., $\pi_{m,m}(n) = d_m(n)\,\forall\, m,\ \forall\, n$, as stated in Sec. 5.1. Therefore, there are only $M(M-1)$ unknown quantities, and there are $2M$ linear equations, M of them involving $\theta_1(n), \ldots, \theta_M(n)$ and M of them involving $\gamma_1(n), \ldots, \gamma_M(n)$, as stated in Eq. (2).

Since a linear system with $2M$ equations and $M(M-1)$ variables is underdetermined (unless $M \leq 3$), we need to impose additional constraints[13] to find the solution. We thus make the following observation: If household orig receives renewable energy during the nth time slot, i.e., if $\gamma_{\mathsf{orig}}(n) > 0$, then $\theta_{\mathsf{orig}}(n) = 0$, since it cannot send and receive power at the same time. If $\theta_{\mathsf{orig}}(n) = 0$, or equivalently, $\sum_{\mathsf{des}\neq\mathsf{orig}}^{M} \pi_{\mathsf{orig},\mathsf{des}}(n) = 0$, then $\pi_{\mathsf{orig},\mathsf{des}}(n) = 0$ for $\mathsf{des} \neq \mathsf{orig}$, because $\pi_{\mathsf{orig},\mathsf{des}}(n) \geq 0,\ \forall\ \mathsf{orig},\ \mathsf{des}$. This means that the linear equations that are homogeneous (i.e., the ones with 0 in their right hand side) allow us to eliminate some of the variables by setting the corresponding elements of the power

[13] We can use the non-linear constraints $\pi_{\mathsf{orig},\mathsf{des}}(n)\pi_{\mathsf{des},\mathsf{orig}}(n) = 0$ directly. However, we would have to examine $2^{\frac{M(M-1)}{2}}$ candidate solutions, which can be computationally expensive.

transfer matrix $\Pi(n,:,:)$ to 0. In fact, after considering all[14] the M homogeneous equations, we are left with $\frac{M^2}{4}$ variables at most. This result is presented in the following Proposition:

Proposition 1. *Let $M \in \mathbb{N}$, and $\mathbf{A}$ be an $M \times M$ matrix. Then, the largest number of elements left in the matrix after removing $x \in \{0, 1, \ldots, M\}$ columns and $M - x$ rows is $\frac{M^2}{4}$.*

Proof. Let x denote the number of removed columns, and $M-x$ be the number of removed rows. The total number of elements left in the matrix after removing x columns and $M - x$ rows is $\kappa(x) = M^2 - Mx - (M - x)^2$, since each column removes M elements, and each row removes $(M - x)$ new elements (x elements were removed when the x columns were crossed-out). $\kappa(x)$ is concave in x and equals 0 when $x = 0$ or $x = M$. The maximum value of $\kappa(x)$ can be obtained by setting $\frac{d}{dx}\kappa(x) = 0$. Therefore, the number of elements left in the matrix is the largest when $x = \frac{M}{2}$. Moreover, $\kappa\left(\frac{M}{2}\right) = \frac{M^2}{4}$. ■

The variables eliminated by the conditions $\gamma_{\mathsf{orig}}(n)\theta_{\mathsf{orig}}(n) = 0,\ \forall\ \mathsf{orig}$ are the same $\pi_{\mathsf{orig},\mathsf{des}}(n)$'s which should be set to zero, following the constraint $\pi_{\mathsf{orig},\mathsf{des}}(n)\pi_{\mathsf{des},\mathsf{orig}}(n) = 0$. The resulting system may still be under-determined. However, under the non-negativity constraint (i.e. $\pi_{\mathsf{orig},\mathsf{des}}(n) \geq 0,\ \forall\ \mathsf{orig},\ \mathsf{des}$) we can determine the solution by solving:

$$\begin{aligned} \text{PR0:} \quad & \min_{\boldsymbol{x}} \ \|\mathbf{A}\mathbf{x} - \mathbf{b}\|_2 \\ \text{s.t.} \quad & \mathbf{x} \succeq \mathbf{0}, \end{aligned} \tag{43}$$

where $\mathbf{A}$ is the matrix that captures the interactions between the remaining variables $\pi_{\mathsf{orig},\mathsf{des}}(n)$'s, which are stacked in the column vector $\mathbf{x}$. The non-zero $\gamma_m(n)$ and $\theta_m(n)$ are stacked in the column vector $\mathbf{b}$. PR0 can be solved by using any of the available non-negative least squares algorithms (NNLS), for example, the fast NNLS (FNNLS) [59].

[14] There are $2M$ linear equations, half of which are homogeneous.

References

[1] E. Ratnam, S. Weller, C. Kellett, Central versus localized optimization-based approaches to power management in distribution networks with residential battery storage, International Journal of Electrical Power and Energy Systems 80 (2016) 396–406.

[2] E. Ratnam, S. Weller, C. Kellett, An optimization-based approach to scheduling residential battery storage with solar pv: Assessing customer benefit, Renewable Energy 75 (2015) 123–134.

[3] N. Javaid, I. Ullah, M. Akbar, Z. Iqbal, F. A. Khan, N. Alrajeh, M. S. Alabed, An Intelligent Load Management System With Renewable Energy Integration for Smart Homes, IEEE Access 5 (2017) 13587 – 13600.

[4] S. C. Chan, K. M. Tsui, H. C. Wu, Y. Hou, Y. Wu, F. F. Wu, Load/price forecasting and managing demand response for smart grids: Methodologies and challenges, IEEE Signal Processing Magazine 29 (5) (2012) 68–85.

[5] I. Ranaweera, O.-M. Midtgård, Optimization of operational cost for a grid-supporting pv system with battery storage, Renewable Energy 88 (2016) 262–272.

[6] P. Harsha, M. Dahleh, Optimal Management and Sizing of Energy Storage Under Dynamic Pricing for the Efficient Integration of Renewable Energy, IEEE Trans. Power Systems 30 (3) (2015) 1164 – 1181.

[7] F. Vieira, P. Moura, A. de Almeida, Energy storage system for self-consumption of photovoltaic energy in residential zero energy buildings, Renewable Energy 103 (2017) 308–320.

[8] I. Ranaweera, O.-M. Midtgård, M. Korpås, Distributed control scheme for residential battery energy storage units coupled with pv systems, Renewable Energy 113 (2017) 1099–1110.

[9] J. Coughlin, J. Grove, L. Irvine, J. F. Jacobs, S. J. Phillips, A. Sawyer, J. Wiedman, A guide to community shared solar: Utility, private, and non-profit project development, Tech. rep., National Renewable Energy Laboratory (May 2012).

[10] G. Ye, G. Li, D. Wu, X. Chen, Y. Zhou, Towards Cost Minimization With Renewable Energy Sharing in Cooperative Residential Communities, IEEE Access (2017) 11688 – 11699.

[11] M. Rastegar, M. Fotuhi-Firuzabad, H. Zareipour, M. Moeini-Aghtaie, A Probabilistic Energy Management Scheme for Renewable-Based Residential Energy Hubs, IEEE Trans. Smart Grid 8 (2016) 2217 – 2227.

[12] D. Wu, H. Zeng, C. Lu, B. Boulet, Two-Stage Energy Management for Office Buildings With Workplace EV Charging and Renewable Energy, IEEE Trans. Transportation Electrification 3 (1) (2017) 225–237.

[13] V. Pilloni, A. Floris, A. Meloni, L. Atzori, Smart Home Energy Management Including Renewable Sources: A QoE-driven Approach, IEEE Trans. Smart Grid 9 (2017) 2006 – 2018.

[14] J. Rajasekharan, V. Koivunen, Optimal Energy Consumption Model for Smart Grid Households With Energy Storage, IEEE J. of Sel. Topics in Signal Process. 8 (6) (2014) 1154–1166.

[15] J. Leithon, T. J. Lim, S. Sun, Online demand response strategies for non-deferrable loads with renewable energy, IEEE Transactions on Smart Grid 9 (5) (2018) 5227–5235.

[16] M. H. Albadi, E. F. El-Saadany, Demand response in electricity markets: An overview, in: 2007 IEEE Power Engineering Society General Meeting, 2007, pp. 1–5.

[17] C. G. Codemo, T. Erseghe, A. Zanella, Energy storage optimization strategies for smart grids, in: 2013 IEEE Int. Conf. on Commun., 2013, pp. 4089–4093.

[18] X. Cao, J. Zhang, H. V. Poor, Joint energy procurement and demand response towards optimal deployment of renewables, IEEE Journal of Selected Topics in Signal Processing 12 (4) (2018) 657–672.

[19] S. Sun, M. Dong, B. Liang, Cost-minimizing distributed algorithm for managing renewable-integrated power grids, in: 2015 IEEE Global Conference on Signal and Information Processing (GlobalSIP), 2015, pp. 987–991.

[20] V. Mohan, R. Suresh, J. G. Singh, W. Ongsakul, N. Madhu, Microgrid Energy Management Combining Sensitivities, Interval and Probabilistic Uncertainties of Renewable Generation and Loads, IEEE J. Emerging and Sel. Topics in Circuits and Systems 7 (2) (2017) 262–270.

[21] Q. Wei, F. L. Lewis, G. Shi, R. Song, Error-Tolerant Iterative Adaptive Dynamic Programming for Optimal Renewable Home Energy Scheduling and Battery Management, IEEE Trans. Industrial Electronics 64 (2017) 9527 – 9537.

[22] Z. Zhou, F. Xiong, B. Huang, C. Xu, R. Jiao, B. Liao, Z. Yin, J. Li, Game-Theoretical Energy Management for Energy Internet With Big Data-Based Renewable Power Forecasting, IEEE Access 5 (2017) 5731–5746.

[23] M. Marzband, M. Javadi, J. L. Domínguez-García, M. M. Moghaddam, Non-cooperative game theory based energy management systems for energy district in the retail market considering DER uncertainties, IET Generation, Transmission Distribution 10 (12) (2016) 2999–3009.

[24] W. Tushar, J. A. Zhang, C. Yuen, D. B. Smith, N. U. Hassan, Management of Renewable Energy for a Shared Facility Controller in Smart Grid, IEEE Access 4 (2016) 4269–4281.

[25] T. C. Chiu, Y. Y. Shih, A. C. Pang, C. W. Pai, Optimized Day-Ahead Pricing With Renewable Energy Demand-Side Management for Smart Grids, IEEE Internet of Things J. 4 (2) (2017) 374–383.

[26] Y. Xiang, J. Liu, Y. Liu, Robust Energy Management of Microgrid With Uncertain Renewable Generation and Load, IEEE Trans. Smart Grid 7 (2) (2016) 1034–1043.

[27] Q. Fu, A. Nasiri, V. Bhavaraju, A. Solanki, T. Abdallah, D. C. Yu, Transition Management of Microgrids With High Penetration of Renewable Energy, IEEE Trans. Smart Grid 5 (2) (2014) 539–549.

[28] K. Rahbar, J. Xu, R. Zhang, Real-Time Energy Storage Management for Renewable Integration in Microgrid: An Off-Line Optimization Approach, IEEE Trans. Smart Grid 6 (1) (2015) 124–134.

[29] H. Lee, C. Tekin, M. van der Schaar, J. Lee, Adaptive contextual learning for unit commitment in microgrids with renewable energy sources, IEEE Journal of Selected Topics in Signal Processing 12 (4) (2018) 688–702.

[30] N. R. Tummuru, M. K. Mishra, S. Srinivas, Dynamic Energy Management of Renewable Grid Integrated Hybrid Energy Storage System, IEEE Trans. Industrial Electronics 62 (12) (2015) 7728–7737.

[31] S. Pannala, N. Padhy, P. Agarwal, Peak Energy Management using Renewable Integrated DC Microgrid, IEEE Trans. Smart Grid 9 (2017) 4906 – 4917.

[32] Z. Zhang, N. Rahbari-Asr, M. Y. Chow, Asynchronous distributed cooperative energy management through gossip-based incremental cost consensus algorithm, in: 2013 North American Power Symposium (NAPS), 2013, pp. 1–6.

[33] I. Stoyanova, M. Biglarbegian, A. Monti, Cooperative energy management approach for short-term compensation of demand and generation variations, in: 2014 IEEE Int. Systems Conf. Proceedings, 2014, pp. 559–566.

[34] A. C. Luna, N. L. Diaz, M. Graells, J. C. Vasquez, J. M. Guerrero, Cooperative energy management for a cluster of households prosumers, IEEE Trans. Consumer Electronics 62 (3) (2016) 235–242.

[35] F. Mangiatordi, E. Pallotti, D. Panzieri, L. Capodiferro, Multi agent system for cooperative energy management in microgrids, in: 2016 IEEE 16th Int. Conf. on Environment and Electrical Engineering (EEEIC), 2016, pp. 1–5.

[36] K. Rahbar, C. C. Chai, R. Zhang, Energy Cooperation Optimization in Microgrids with Renewable Energy Integration, IEEE Trans. Smart Grid 9 (2016) 1482 – 1493.

[37] H. Dagdougui, A. Ouammi, L. Dessaint, R. Sacile, Global energy management system for cooperative networked residential green buildings, IET Renewable Power Generation 10 (8) (2016) 1237–1244.

[38] Y. Zhang, N. Rahbari-Asr, J. Duan, M. Y. Chow, Day-Ahead Smart Grid Cooperative Distributed Energy Scheduling With Renewable and Storage Integration, IEEE Trans. Sustainable Energy 7 (4) (2016) 1739–1748.

[39] Z. Wang, C. Gu, F. Li, Flexible operation of shared energy storage at households to facilitate pv penetration, Renewable Energy 116 (2018) 438–446.

[40] M. Marzband, F. Azarinejadian, M. Savaghebi, E. Pouresmaeil, J. M. Guerrero, G. Lightbody, Smart transactive energy framework in grid-connected multiple home microgrids under independent and coalition operations, Renewable Energy 126 (2018) 95–106.

[41] T. Li, M. Dong, Real-time energy storage management with renewable integration: Finite-time horizon approach, IEEE J. on Sel. Areas in Communications 33 (12) (2015) 2524–2539.

[42] L. Yu, T. Jiang, Y. Zou, Online energy management for a sustainable smart home with an hvac load and random occupancy, IEEE Trans. Smart Grid 10 (2017) 1646 – 1659.

[43] T. Li, M. Dong, Real-time residential-side joint energy storage management and load scheduling with renewable integration, IEEE Trans. Smart Grid 9 (1) (2018) 283–298.

[44] T. Li, M. Dong, Residential energy storage management with bidirectional energy control, IEEE Trans. Smart Grid 10 (2018) 3596 – 3611.

[45] T. Li, M. Dong, Real-time energy storage management: Finite-time horizon approach, in: 2014 IEEE International Conference on Smart Grid Communications (SmartGridComm), 2014, pp. 115–120.

[46] L. Yu, T. Jiang, Y. Zou, Distributed online energy management for data centers and electric vehicles in smart grid, IEEE Internet of Things J. 3 (6) (2016) 1373–1384.

[47] W. Shi, N. Li, C. C. Chu, R. Gadh, Real-time energy management in microgrids, IEEE Trans. Smart Grid 8 (1) (2017) 228–238.

[48] B. Li, T. Chen, X. Wang, G. B. Giannakis, Real-time energy management in microgrids with reduced battery capacity requirements, IEEE Trans. Smart Grid 10 (2017) 1928 – 1938.

[49] H. Yin, C. Zhao, C. Ma, Decentralized real-time energy management for a reconfigurable multiple-source energy system, IEEE Trans. Industrial Informatics 14 (2018) 4128 – 4137.

[50] M. S. Taha, H. H. Abdeltawab, Y. A. R. I. Mohamed, An online energy management system for a grid-connected hybrid energy source, IEEE J. of Emerging and Sel. Topics in Power Electronics 6 (2018) 2015 – 2030.

[51] E. Dall'Anese, A. Bernstein, A. Simonetto, Feedback-based projected-gradient method for real-time optimization of aggregations of energy resources, in: 2017 IEEE Global Conference on Signal and Information Processing (GlobalSIP), 2017, pp. 1040–1044.

[52] C. Jin, X. Sheng, P. Ghosh, Optimized electric vehicle charging with intermittent renewable energy sources, IEEE Journal of Selected Topics in Signal Processing 8 (6) (2014) 1063–1072.

[53] T. Chen, X. Wang, G. B. Giannakis, Energy and workload management for data centers in renewable-integrated power grid, in: 2015 IEEE Global Conference on Signal and Information Processing (GlobalSIP), 2015, pp. 513–517.

[54] A. C. Luna, L. Meng, N. L. Diaz, M. Graells, J. C. Vasquez, J. M. Guerrero, Online energy management systems for microgrids: Experimental validation and assessment framework, IEEE Trans. Power Electronics 33 (3) (2018) 2201–2215.

[55] E. Hooshmand, A. Rabiee, Energy management in distribution systems, considering the impact of reconfiguration, ress, esss and dr: A trade-off between cost and reliability, Renewable Energy 139 (2019) 346–358.

[56] N. Karmarkar, A new polynomial-time algorithm for linear programming, Combinatorica 4 (4) (1984) 373–395.

[57] S. Nagar, Introduction to Scilab: For Scientists and Engineers, Independently published, 2016.

[58] S. Boyd, L. Vandenberghe, Convex Optimization, Cambridge University Press, New York, NY, USA, 2004.

[59] R. Bro, S. De Jong, A fast non-negativity-constrained least squares algorithm, J. of Chemometrics 11 (5) (1997) 393–401.

[60] Southern California Edison, TOU-GS-2-RTP General service-medium real time pricing, Accessed June 2018 (2018).
URL `https://www.sce.com/NR/sc3/tm2/pdf/CE331.pdf`

[61] National Renewable Energy Laboratory, PVWatts calculator, Accessed June 2018 (2018).
URL `http://pvwatts.nrel.gov`

[62] H. Shiraki, S. Nakamura, S. Ashina, K. Honjo, Estimating the hourly electricity profile of japanese households – coupling of engineering and statistical methods, Energy 114 (2016) 478–491.